2008

Mixed Lubrication Analysis of Vane Sliding Surface in Rotary Compressor Mechanisms - Influences of Elastic Deformation at Surface End of Vane Slot -

Yasutaka Ito
Toshiba Corporation

Hitoshi Hattori
Toshiba Corporation

Kazuhiko Miura
Toshiba Corporation

Mixed Lubrication Analysis of Vane Sliding Surface in Rotary Compressor Mechanisms - Influences of Elastic Deformation at Surface End of Vane-slot -

Yasutaka Ito[1], Hitoshi Hattori[2], Kazuhiko Miura[3]

[1, 2] Corporate Research & Development Center, Toshiba Corporation
1, Komukai toshiba-cho, Saiwai-ku, Kawasaki 212-8582, Japan
Tel: +81-44-549-2380, Fax: +81-44-549-2383
E-mail: yasutaka.ito@toshiba.co.jp
E-mail: hit.hattori@toshiba.co.jp

[3] Toshiba Carrier Corporation
336, Tadehara, Fuji-shi, Shizuoka-ken 416-8521, Japan
Tel: +81-545-62-5591, Fax: +81-545-66-0305
E-mail: kazuhiko2.miura@toshiba.co.jp

ABSTRACT

In order to investigate the effects of the elastic deformation of the vane-slot on the lubrication characteristics of the vane sliding surface in a rotary compressor, a mixed lubrication analysis considering the elastic deformation has been performed for the vane sliding surface. In this analysis, the modified Reynolds equation and the elastic contact equation, within which the influence of surface roughness is considered, are solved as a coupled problem. The elastic deformation of the vane-slot is calculated by using an FEM model with two dimensional iso-parametric elements. By comparing the analysis results with that of a rigid-body model, the effects of the elastic deformation of the vane-slot on the lubrication characteristics were made clear. As a result, it is found that the elastic deformation should be considered in the analysis model of mixed lubrication between the vane and the vane-slot.

1. INTRODUCTION

In the compression mechanism of a rotary compressor for air conditioners, a vane is provided to separate the suction chamber and the compression chamber. The vane which undergoes reciprocating motion is driven by the eccentric rotation of the rolling piston. Severe load and moment generated by the pressure difference between the suction chamber and the compression chamber act on the vane and the vane-slot. When the friction loss and the surface damage of the vane increase, the performance and the reliability of the rotary compressors will decrease. Therefore, the optimum design by which a good lubricating condition on the sliding surface of the vane can be realized is required. In a previous study(1), in order to realize the optimum design of the vane, a numerical analysis approach for mixed lubrication has been developed. In the analysis, the vane-slot was assumed as a rigid body. However, solid contact may occur at the surface end of vane-slot, and the elastic deformation of the surface end may become large. So, it is considered that the elastic deformation of vane-slot may influence the lubrication characteristics of vane sliding surface. In order to investigate the effects of the elastic deformation on the lubrication characteristics, a mixed lubrication analysis considering the elastic deformation has been performed for the vane sliding surface. The modified Reynolds equation and the elastic contact equation, within which the influence of

surface roughness is considered, are solved as a coupled problem. The elastic deformation of the vane-slot is calculated by using an FEM model with two dimensional iso-parametric elements. The occurrence of solid contact in the hydrodynamic lubrication film can be predicted by the analysis technology. Based on the predicted conditions of solid contact, the damage of the surface and lubrication characteristics are evaluated. In this paper, at first, the governing equations and the procedures of analysis are described. Next, the analysis results of the elastic deformation model and the rigid body model are shown. Finally, by comparing the analysis results, the effects of the elastic deformation on the lubrication characteristics were made clear.

2. GOVERNING EQUATIONS

Figure 1 shows a brief drawing of the compression mechanism in a rotary compressor. The rolling piston which is driven by the crank rotates eccentrically. Due to this eccentric rotation, the volume of the compression chamber decreases, and the pressure of refrigerant becomes high. The vane separates the suction chamber and the compression chamber. Figure 2 shows the coordinate system of vane.

2.1 Equations of Motion of Vane

As shown in Fig.1, the vane is subjected to the load due to the differences of pressures, the spring force, the friction forces between vane and vane-slot and the friction force between vane and rolling piston. The equation of motion of the vane and the equations of equilibrium of forces and moments are [2, 3],

$$m_v \ddot{x}_v = F_{vx} + F_{t1} + F_{t2} + F_{vn}\cos\alpha + F_{vt}\sin\alpha - F_s \tag{1}$$

$$0 = F_{vy} + F_{c1} - F_{c2} + F_{vt}\cos\alpha - F_{vn}\sin\alpha + w_c\int p_1 dx - w_c\int p_2 dx \tag{2}$$

$$0 = M_{vt} + M_{t1} - M_{t2} + M_{c1} - M_{c2} + M_v + w_c\int x p_1 dx - w_c\int x p_2 dx \tag{3}$$

where m_v is the mass of vane, x_v is the displacement of vane along x direction, α is the angle extended by piston and vane contact point, w_c is the width of cylinder, p_1 and p_2 are the oil film pressures between vane and vane-slot corresponding to the discharge side and the suction side, F_{vx}, F_{vy} and M_v are the forces and moment acting on vane due to the refrigerant pressure difference, F_{t1}, F_{t2}, M_{t1} and M_{t2} are the friction forces and the corresponding moments between vane and vane-slot, F_{c1}, F_{c2}, M_{c1} and M_{c2} are the contact forces and the corresponding moments between vane and vane-slot, F_{vn} is the normal force acting on vane at piston contact, F_{vt} and M_{vt} are the friction force and the corresponding moment acting on vane at piston contact, F_s is the spring force.

2.2 Reaction Forces of Oil Film between Vane and Vane Slot

The vane sliding surface is treated as a surface having infinite width along the perpendicular of the plane of Fig.2. The reaction forces of oil film on discharge side and suction side between the vane and vane-slot are calculated by the modified Reynolds equations as follows [4],

$$\frac{\partial}{\partial x}\left(\Phi_X \frac{\bar{h}^3}{\eta}\frac{\partial p}{\partial x}\right) = 6U\frac{\partial h_T}{\partial x} + 6U\sigma\frac{\partial \Phi_s}{\partial x} + 12\frac{\partial h_T}{\partial t} \tag{4}$$

where $\bar{h}$ is the average oil film thickness, h_T is the local oil film thickness, η is the oil viscosity, U is the sliding velocity of vane, σ is the standard deviations of composite roughness, Φ_X is the pressure flow factor, Φ_s is the shear flow factor. The local oil film thickness h_T is expressed as follows.

$$h_T = \frac{\bar{h}}{2}\left\{1 + erf\left(\frac{\bar{h}}{\sqrt{2}\sigma}\right)\right\} + \frac{\sigma}{\sqrt{2\pi}}\exp\left(-\frac{1}{2}\left(\frac{\bar{h}}{\sigma}\right)^2\right) \tag{5}$$

The oil film thickness on discharge side and suction side between the vane and vane-slot are,

$$\overline{h}_1 = c_g - \overline{h}_0 - kx \quad (6)$$

$$\overline{h}_2 = \overline{h}_0 + kx + \delta \quad (7)$$

where, $\overline{h}_1$ and $\overline{h}_2$ are the average oil film thicknesses on discharge side and suction side, c_g is the clearance between vane and vane slot, $\overline{h}_0$ is the average oil film thickness at the lower end of vane slot (x=0 location in Fig. 2) on suction side, k is the inclination of vane. In $\overline{h}_2$, the elastic deformation of the vane-slot δ is considered.

2.3 Contact Forces between Vane and Vane slot

For calculating the contact forces between the vane and the vane slot, the Patir and Cheng's approximate expression based on Greenwood and Tripp's theory are used [5, 6],

$$p_c = \begin{cases} k_c E' \times 4.4086 \times 10^{-5} \left(4 - \dfrac{\overline{h}}{\sigma}\right)^{6.804} & \left(\overline{h} < 4\sigma\right) \\ 0 & \left(\overline{h} \geq 4\sigma\right) \end{cases} \quad (8)$$

where, p_c is the contact pressure between the vane and vane slot, k_c is a constant in force-compliance relationship, E' is the equivalent elastic modulus.

2.4 Elastic Deformation of Vane-slot on Suction side

In this analysis, the elastic deformation of vane-slot on suction side is calculated by using FEM. As shown in Fig. 3, mesh division of cylinder on suction side is carried out. The elastic deformation of node on the vane-slot due to the oil film force and the contact force is calculated. The elastic deformation of vane-slot δ is expressed as follows.

$$\delta = u_y \quad (9)$$

where, u_x, u_y are the coordinates of elastically deformed surface of vane-slot. The displacement vector $\{u\}$ containing u_x and u_y is expressed as follows.

$$\{u\} = [C]\{f\} \quad (10)$$

where, $[C]$ is the Influence coefficient matrix, $\{f\}$ is the external load vector acting on nodes which is calculated from the pressure distribution on the vane-slot. $[C]$ is the inverse matrix of the rigid matrix $[K]$ of the FEM model[7].

3. ANALYSIS PROCEDURE AND CONDITIONS

3.1 Analysis Procedure

Eqs. (1)-(3), (4), (8) and Eq. (10) are solved as a coupled problem, and the oil film force of vane sliding surface, contact force between the vane and vane-slot, and elastic deformation of vane-slot are calculated. Moreover, the variations of the forces and the moments acting on vane are considered. Consequently, the coupled problem becomes time variant, and is solved recursively along the time axis.

3.2 Analysis conditions

The analysis conditions are shown in Table 1. The radius of cylinder is 31.5mm. The outer radius of rolling piston is 26.2mm. The eccentricity of crank is 5.3mm. The suction pressure is 1.27MPa. The discharge pressure is 4.25MPa. The rotor rotating frequency is 60Hz. The oil viscosity is 2.83×10^{-3} Pa·s. The material of cylinder is cast-iron. Its material constants are used for the calculation of [C]. In this analysis, the modulus of longitudinal elasticity

is 120GPa, and Poisson's ratio is 0.27. Figure 4 shows the relationship between the crank angle and the pressure of compression chamber, which was used as the analysis condition. It contains the effects of over compression.

4. RESULTS AND DISCUSSION

4.1 Effects of Elastic Deformation

Figure 5 shows the analysis results of the elastic deformation model and the rigid body model. The horizontal axis is the crank angle ψ. Figure 5 (a) shows the variation of the inclination of vane k with respect to the crank angle through one revolution of the crank is shown. It can be seen that k is always larger than 0°. That is, the vane always inclines in the clockwise direction as shown in Fig.2. Consequently, the solid contact between the vane and vane slot occurs at the lower end (x=0 location in Fig. 2) on suction side and at upper end (x=l_v location in Fig. 2) on discharge side. It can be seen that, in the neighborhood of ψ=210° which is the crank angle that k approximately reaches a maximum value, k of the elastic deformation model is larger than that of the rigid body model. This is due to the reason that, the elastic deformation of vane-slot increases at the lower end where the solid contact occurs. Figure 5 (b) shows the variation of the average oil film thickness at the lower end of vane slot on suction side in the form of oil film parameter Λ_0 ($=\overline{h}_0/\sigma$) through one revolution of the crank. Because the inclination k is always larger than 0° as shown in Fig. 5(a), it can be seen from the geometry of vane (Fig. 2) that h_0 becomes the minimum oil film thickness on suction side between the vane and vane slot. It can be seen that Λ_0 increases between ψ=0° to ψ=180°. This is due to the reason that, the oil film pressures on suction side is raised by the wedge film effect. Because the wedge film effect disappears when the motion of vane turns over, Λ_0 decreases drastically from ψ=180°. It can be seen that, in the neighborhood of ψ=210° which is the crank angle that Λ_0 approximately reaches a minimum value, Λ_0 of the elastic deformation model is larger than that of the rigid body model. This is due to the reason that, by considering the effect of elastic deformation, the clearance between the vane and the vane-slot increases at the lower end. The minimum oil film parameter of the elastic deformation model is about twice of that of the rigid body model. Figure 5 (c) shows the variation of reaction forces of oil film per unit width of cylinder w_c on suction side between vane and vane slot through one revolution of the crank. Figure 5 (d) shows the variation of contact forces per unit width of cylinder w_c on suction side between vane and vane slot through one revolution. It can be seen that the lubrication on suction side between the vane and vane slot is in a hydrodynamic lubrication zone from ψ=0° to ψ=180°. From ψ=180°, the reaction forces of oil film on suction side decreases drastically, and thus the contact forces occurs. It can be seen that for the rigid body model, the reaction forces of oil film decrease drastically from ψ=180°, and for the elastic deformation model, the reaction forces of oil film decrease from ψ=210°. Therefore, the contact force of the elastic deformation model is smaller than that of the rigid body model during ψ＝ 180° to 210°. This difference is caused by the wedge film effect and squeeze effect due to the elastic deformation of the vane-slot at the lower end. Figure 5 (e) shows the variation of reaction forces of oil film per unit width of cylinder w_c on discharge side between vane and vane-slot through one revolution of the crank. Figure 5 (f) shows the variation of contact forces per unit width of cylinder w_c on discharge side between vane and vane-slot through one revolution of the crank. There is almost no difference between two models. The influences of the elastic deformation are not obvious.

By considering the elastic deformation, the maximum value of k and the minimum value of Λ_0 increase. And just before the starting moment of discharge, the film formation ability of the vane sliding surface increase and contact forces decrease. The influence of elastic deformation becomes remarkable when the solid contact occurs. Therefore, the mixed lubrication analysis considering elastic deformation is required in order to investigate the lubrication characteristic of the vane sliding surface more exactly.

4.2 Elastic Deformation and Pressure Distribution of Vane Sliding Surface

Figure 6 shows the elastic deformation of the vane-slot on suction side. Figure 7 shows the distributions of oil film pressure and contact pressure at ψ=210°. The horizontal axis is the dimensionless distance X (= x/l_v) along x direction. And, the compression pressure reaches the maximum at ψ=210°. Figure 6 (a) shows the elastic deformation at ψ=0°, 30°, 60°, 90°, 120° and 150°. Figure 6 (b) shows the elastic deformation at ψ=180°, 210°, 240°, 270°, 300° and 330°. It is found that the elastic deformation increases during the period (from ψ=210° to ψ=330°) of the solid contact and at ψ=180° where the reaction force of oil film is large. At ψ=210°, 240°, 270°, the maximum value of the elastic deformation is about 8 times of that of ψ=0°～120°. Figure 7 (a) shows the distributions of oil film pressure and contact pressure of the elastic deformation model. Figure 7 (b) shows the distributions of oil film pressure and contact pressure of the rigid body model. It can be seen that the oil film at the lower end (from X=0 to X=0.2) is not formed in the rigid body model and the load exerted on vane sliding surface is supported by the contact force. Moreover, it is found that, in the elastic deformation model, oil film possessing load carrying capacity exists at the lower end and the oil film pressure is large. As a result, the maximum contact pressure of the elastic deformation model is about 60% of that of the rigid body model.

From the results of Fig. 6 and Fig. 7, it can be seen that the clearance at the lower end increases due to the elastic deformation. And by this effect, the film formation ability of the vane sliding surface increases.

5. CONCLUSION

The mixed lubrication analysis considering the elastic deformation has been performed in order to investigate the effects of elastic deformation of vane-slot on the lubrication characteristics of vane sliding surface in a rotary compressor. As a result, the following conclusions have been obtained.

1. Due to the effects of elastic deformation, the film formation ability of the vane sliding surface increases just before the starting moment of discharge and the contact forces decrease.
2. In the discharge process, as the load carrying capacity of oil film is small and the solid contact is dominant, the elastic deformation of the vane-slot increases.
3. From the results of this study, in order to realize the friction loss reduction and high reliability of the rotary compressor, mixed lubrication analysis considering elastic deformation is required in the optimum design of the vane.

REFERENCES

1. Ito, Y., Hattori, H., Miura, K., Hirayama, T., 2007, Mixed Lubrication Analysis of Vane Sliding Surface in Rotary Compressor Mechanisms, Tribology Online, Vol. 2, No.3, p.73-77. (http://www.jstage.jst.go.jp/article/trol/2/3/2_73/_article)
2. Padhy, S. K., 1993, On the Dynamics of a Rotary Compressor: part1 – Mathematical modeling, Proc. of the A.S.M.E. Design Automation Conference., Vol. 65-1:p. 207-217.
3. Kobayashi, H., Ota Y., 1989, Analysis of Blade Behavior in Rotary Compressor, Mitsubishi Juko Giho., Vol. 26, No. 3:p. 195-199.
4. Patir, N., Cheng, H. S.., 1978, An Average Flow Model for Determining Effects of Three Dimensional Roughness on Partial Hydrodynamic Lubrication, Transaction of the ASME, Journal of Lubrication Technology., Vol. 100, 1:p. 12-17.
5. Greenwood, J. A., Tripp, J. H., 1970, The Contact of Two Nominally Flat Surfaces, Proceeding of the Institution of Mechanical Engineers., Vol. 185, No. 48, p. 625-633.
6. Patir, N., Cheng, H. S., 1978, Effect of surface roughness orientation on the central film thickness in E.H.D. contacts, Proceeding of the Institute of Mechanical Engineering Part I., Vol. 185, No. 48, p. 15-21.
7. Hattori, H., 1998, EHL Analysis of a Journal Bearing for Rotary Compressors under Dynamic Loading, Transactions of the Japan Society of Mechanical Engineers. C, 64(624), p.3171-3178.

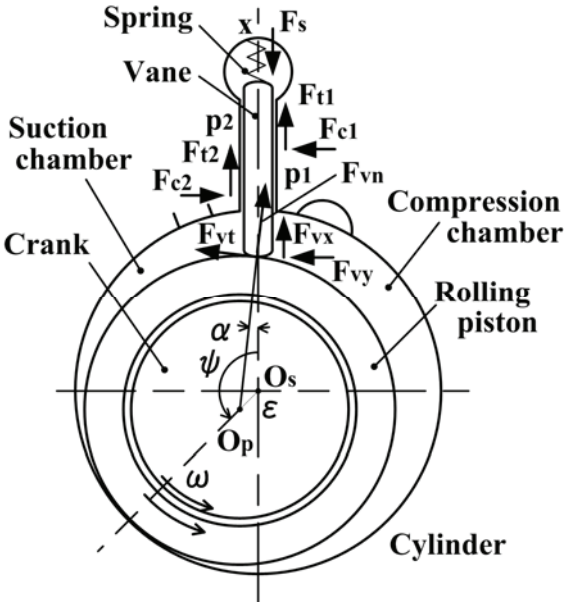

Figure1. Brief drawing of compression mechanism in rotary compressor

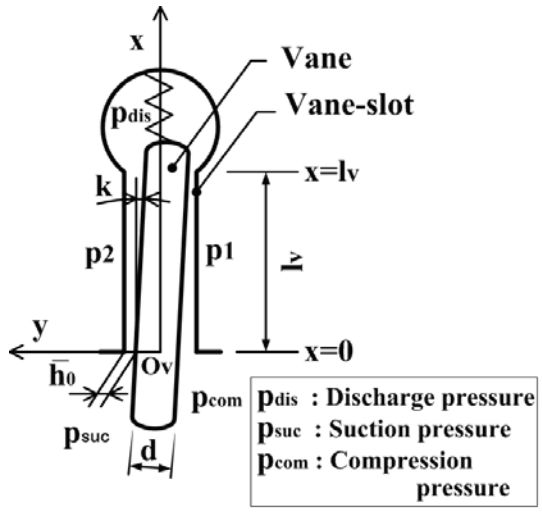

Figure2. Coordinate system of vane

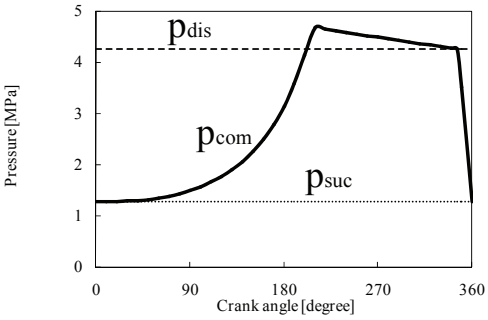

Figure4. Pressure of compression chamber

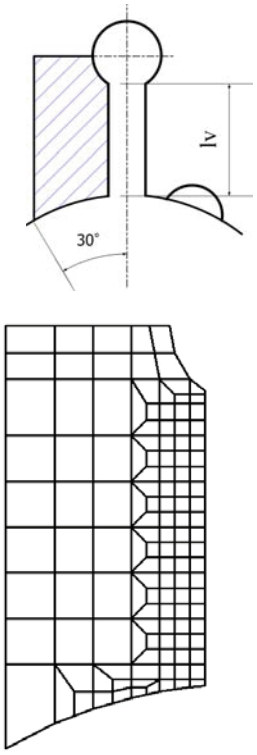

Figure3. FEM model of vane-slot on suction side

Table 1 Analysis conditions

Radius of cylinder [mm]	31.5
Outer radius of piston [mm]	26.2
Eccentricity of crank, ε [mm]	5.3
Dimensionless clearance between vane and vane slot, C_v (= c_v / d) [10^{-3}]	3.96
Dimensionless length of vane slot, L_v (= l_v / d)	3.4
Rotor Rotating Frequency, N [Hz]	60
Discharge pressure, P_{dis} [MPa]	4.25
Suction pressure, P_{suc} [MPa]	1.27
Oil viscosity, η [10^{-3} Pa・s]	2.8
Poisson's ratio of cylinder	0.3
Young's modulus of cylinder [GPa]	120

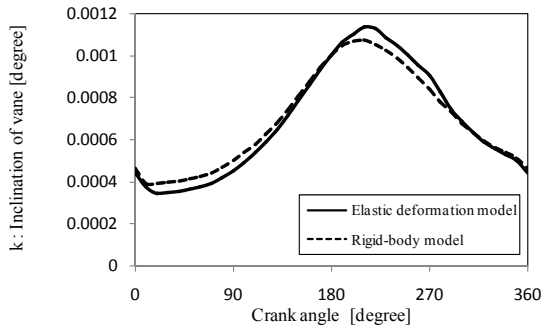

(a) Inclination of vane

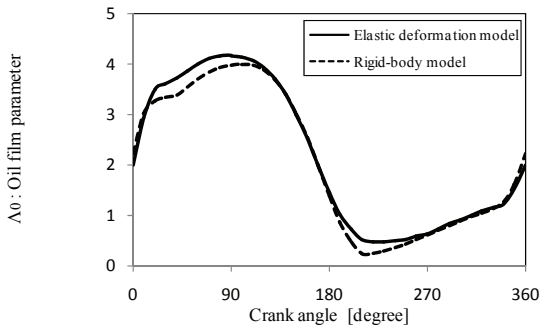

(b) Minimum oil film thickness on suction side

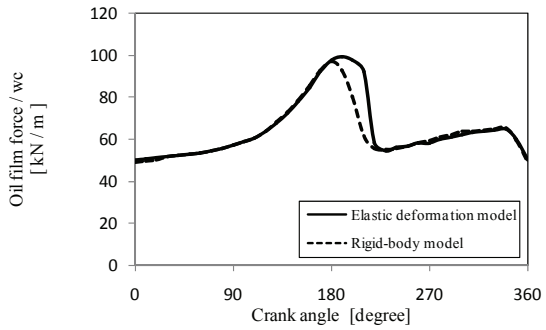

(c) Oil film force on suction side

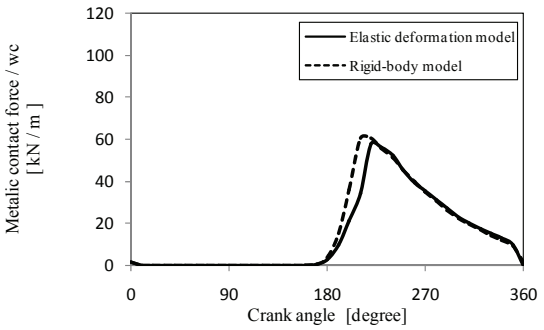

(d) Contact force on suction side

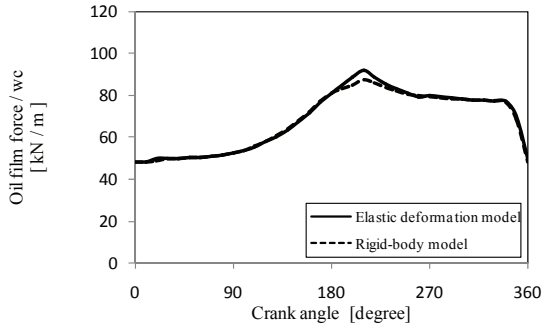

(e) Oil film force on discharge side

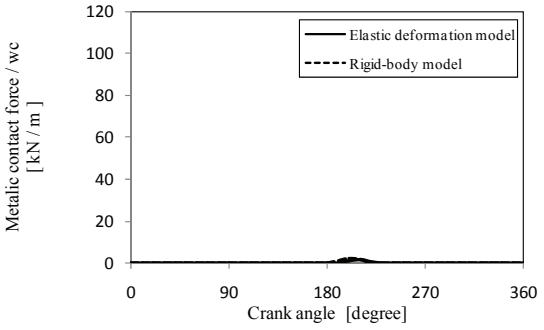

(f) Contact force on discharge side

Figure5. Comparison of Elastic deformation model and Rigid-body model

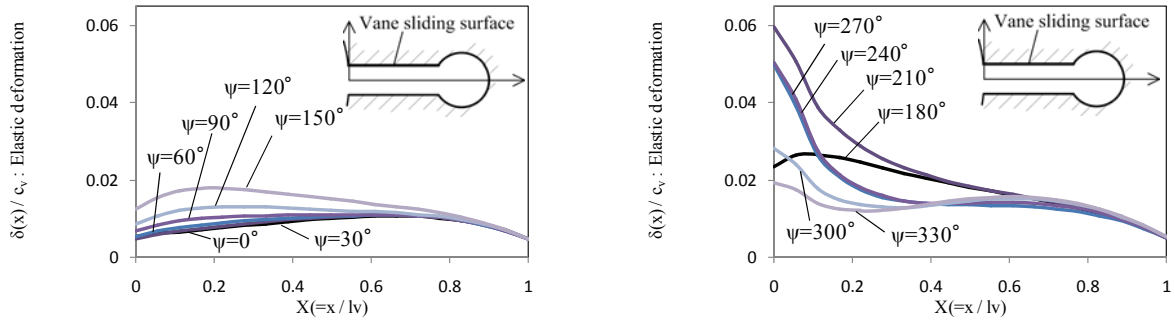

(a) Crank angle:ψ=0° ～150° (b) Crank angle:ψ=180° ～ 330°

Figure6. Elastic deformation of vane sliding surface on suction side (Elastic deformation model)

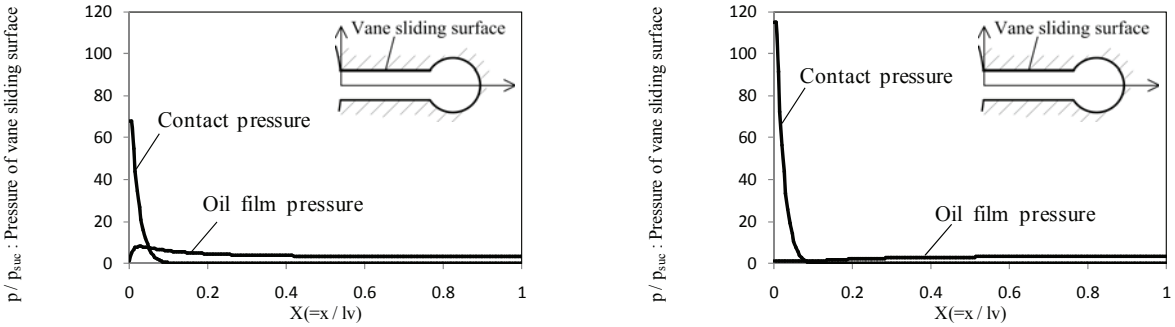

(a) Elastic deformation model (b) Rigid-body model

Figure7. Pressure distribution of vane sliding surface on suction side (Crank angle: ϕ = 210°)